

Resonance enhanced two-photon cavity ring-down spectroscopy of vibrational overtone bands: a proposal

Kevin K. Lehmann^{1, a)}

*Departments of Chemistry and Physics, University of Virginia, Charlottesville VA,
22904-4319*

(Dated: 15 April 2022)

This paper presents an analysis of near-resonant, ro-vibrational two-photon spectroscopy and use of cavity ring-down spectroscopy for its detection. An expression is derived for the photon absorption rate of a three level system, correct to all orders and the simpler expressions that result from various approximations. Account is made for spatial degeneracy and linear or circular polarization of the exciting field. Expressions are derived for the rate of two-photon power loss for light inside a resonant cavity. Explicit calculations are made for excitation of the ν_3 mode of $^{12}\text{C}^{16}\text{O}_2$ where it is found that the two-photon excitation spectrum is dominated by a single $Q(16)$ at $\tilde{\nu} = 2335.826 \text{ cm}^{-1}$ line which has an intermediate $P(16)$ one-photon transition that is off resonance by 0.093 cm^{-1} (2.8 GHz). At 1 torr total pressure, two-photon cross section of $7.48 \cdot 10^{-39} \text{ cm}^4\text{s}$ per CO_2 molecule in the $J = 16$ state or $5.61 \cdot 10^{-40} \text{ cm}^4\text{s}$ per CO_2 molecule is calculated. Based upon an analysis of the sensitivity limits for 2-photon cavity ring-down spectroscopy, a theoretical detection limit of 22 ppq (10^{-15}) $\text{Hz}^{-1/2}$ for $^{12}\text{C}^{16}\text{O}_2$ is predicted, higher sensitivity than has been realized using one-photon absorption. It is predicted that most polyatomic molecules will have sparse, Doppler-Free two-photon absorption spectra which will dramatically increase the selectivity of trace gas detection of samples with multiple components with overlapping absorption bands.

^{a)}Electronic mail: lehmann@virginia.edu

Trace gas detection has been revolutionized by the use of low-loss optical cavity enhanced spectroscopic methods. Starting with the introduction of the Cavity Ring-down technique in 1988,¹ many forms of cavity enhanced spectroscopies (CES) have been developed and used for a wide range of applications.^{2,3} Most of these papers have involved detection of gases, though applications for liquids^{4,5} and surfaces⁶⁻⁸ also are common. Essentially all prior work has involved one-photon spectroscopy, in either the linear or saturated absorption regime. One of the most impressive achievements has been development of instruments to measure $^{14}\text{C}^{16}\text{O}_2$ in pure CO_2 samples,⁹ with a sensitivity of 5 ppq (mole fraction in parts per 10^{15}) after 2 hours of integration, well below the ~ 1 ppt fractional abundance of ^{14}C for atmospheric CO_2 . There are several scientific instrument companies that specialize in CES based trace gas analyzers. The principle advantage of using CES approaches is that one gets an effective absorption path-length that is $(1 - R_M)^{-1}$ (where R_M is the mirror reflectivity) times larger than the physical length of the cell. In the near-IR through most of the visible spectral range, mirrors with enhancements of $\sim 10^5$ are commercially available.

In trace detection, both sensitivity and selectivity are key. The use of CES allows for remarkable sensitivity, but in one-photon absorption, the selectivity is limited by high density of weak transitions of the principle components of the gas if they are polyatomic molecules. One can minimize the overlap by pressure broadened tails of other transitions by working at pressures where the lines are Doppler broadened, but that compromises sensitivity. Also, given the high enhancement of the power inside the sample cavity compared to the output power, one can have optical saturation of the detection transition(s) at cavity output powers that give signals on the detectors only modestly higher than detector noise.¹⁰ This is particularly problematic when doing sensing with Mid-IR radiation, where the molecular transitions are strong but the detectors have limited sensitivity. The rate of absorption, in the case of saturation, is limited by the fraction of the density of molecules interacting with the light. This fraction equals the fractional population of the lower state of the transition times the ratio of the power broadened homogeneous to the total transition width. Optical saturation has an advantage in that the saturating part of the cavity loss does not give an exponential decay, which is exploited in the Saturated-Absorption Cavity Ring-Down Spectroscopy (SCARS) technique¹¹ to distinguish it from the nonsaturated contributions of cavity loss, though the two loss contributions remain highly correlated.¹²

In this paper, I discuss a novel approach to CES that utilizes near-resonant, degenerate rovibrational two-photon absorption (TPA) by the gas contained in a low loss optical cavity. De-

generate two-photon absorption from counter-propagating optical fields is intrinsically Doppler-Free,¹³⁻¹⁵ therefore, regardless of thermal velocity, all molecules in the correct lower state will absorb in a transition with frequency width limited by the homogeneous width of the transition.¹³ The unsaturated, peak absorption strength of TPA will saturate as a function of pressure once the homogeneous width due to pressure broadening exceeds the transit time broadening, which is typically only ~ 100 kHz. Biraben recently reviewed the early work in Doppler-Free two-photon spectroscopy.¹⁶

I. THREE LEVEL OPTICAL BLOCH EQUATION, WITH ALL RELAXATION RATES = γ

The theory of two-photon absorption has been traditionally treated using second order, time dependent perturbation theory.¹⁷⁻¹⁹ In the electric dipole approximation, the rate of two-photon excitation from state 1 to 3 by absorption of two-photons of angular frequency $\omega = (E_3 - E_1)/2\hbar$ can be shown to be proportional to the square of an amplitude, $S_{13}^{(2)}$, that itself can be written in terms of a sum over virtual intermediate states, 2,¹⁹

$$S_{13}^{(2)} = \sum_2 \frac{\mu_{12}\mu_{23}}{E_2 - E_1 - \hbar\omega + i\hbar\gamma_{12}} \quad (1)$$

where μ_{12} and μ_{23} are the transition electric dipole moments between the three states projected on the polarization direction of the driving electric field and γ_{12} is the dephasing rate for the $1 \leftrightarrow 2$ transition. It is evident that there is a resonance enhancement when there is a state 2 that has allowed transitions to both states 1 and 3 and is nearly half way between these states such that $E_2 - E_1 - \hbar\omega \approx 0$. This is the case we will be considering in this work and we will assume that one particular such state 2 dominates the sum for $S_{13}^{(2)}$. However, in this case, it is possible for the system to be driven sufficiently hard that the perturbation treatment is no longer accurate. For the case of a single nearly resonant intermediate state, one can derive steady state solutions to the density matrix of the driven three level system and this allows for calculation of the photon absorption rate for arbitrary excitation conditions, which is done below.

Consider a three level system, with states labeled 1, 2, 3 with optical transitions between states $1 \leftrightarrow 2$ and $2 \leftrightarrow 3$ with definitions $\Omega_{12} = \mu_{12}\mathcal{E}/2\hbar$, $\Omega_{23} = \mu_{23}\mathcal{E}/2\hbar$ where \mathcal{E} is the optical electric field amplitude at the position of the molecule, and $\hbar\Delta\omega_{12} = E_2 - E_1 - \hbar\omega$ where E_2 and E_1 are the energy of states 1 and 2, and the corresponding definition for $\Delta\omega_{13}$. We will assume that at

equilibrium only state 1 is populated and all collisional relaxation rates are equal to γ . Under these assumptions, along with the rotating wave approximation, we can write the time evolution of the components of the density matrix as:²⁰

$$\begin{aligned}
-\dot{\rho}_{11} &= \gamma(\rho_{11} - 1) + i\Omega_{12}^* \rho_{12} - i\Omega_{12} \rho_{21} \\
-\dot{\rho}_{22} &= \gamma\rho_{22} - i\Omega_{12}^* \rho_{12} + i\Omega_{12} \rho_{21} + i\Omega_{23}^* \rho_{23} - i\Omega_{23} \rho_{32} \\
-\dot{\rho}_{33} &= \gamma\rho_{33} - i\Omega_{23}^* \rho_{23} + i\Omega_{23} \rho_{32} \\
-\dot{\rho}_{12} &= -\dot{\rho}_{21}^* = i\Omega_{12}(\rho_{11} - \rho_{22}) + (\gamma - i\Delta\omega_{12})\rho_{12} + i\Omega_{23}^* \rho_{13} \\
-\dot{\rho}_{13} &= -\dot{\rho}_{31}^* = i\Omega_{23} \rho_{12} + (\gamma - i\Delta\omega_{13})\rho_{13} - i\Omega_{12} \rho_{23} \\
-\dot{\rho}_{23} &= -\dot{\rho}_{32}^* = -i\Omega_{12}^* \rho_{13} + i\Omega_{23}(\rho_{22} - \rho_{33}) + (\gamma + i(\Delta\omega_{12} - \Delta\omega_{13}))\rho_{23}
\end{aligned} \tag{2}$$

The steady state rate of photon absorption per molecule is given by $R_{ss} = \gamma(\rho_{22} + 2\rho_{33})$. The full steady state solution for R_{ss} (derived using Mathematica) is

$$\begin{aligned}
R_{ss} &= 2\gamma|\Omega_{12}|^2 \left(|\Omega_{12}|^4 + 7|\Omega_{23}|^4 + 2|\Omega_{23}|^2 \left(\gamma^2 + 4|\Omega_{23}|^2 + (\Delta\omega_{12} - \Delta\omega_{13})\Delta\omega_{13} \right) \right. \\
&+ \left(\gamma^2 + (\Delta\omega_{12} - \Delta\omega_{13})^2 \right) \left(\gamma^2 + \Delta\omega_{13}^2 \right) + [\Omega_{23}|^2 (8\gamma^2 + 2\Delta\omega_{12}^2 - 3\Delta\omega_{12}\Delta\omega_{13} + 6\Delta\omega_{13}^2) \Big/ \\
&\left[4|\Omega_{12}|^6 + |\Omega_{12}|^4 \left(9\gamma^2 + 12|\Omega_{23}|^2 + \Delta\omega_{12}^2 + 8\Delta\omega_{12}\Delta\omega_{13} - 8\Delta\omega_{13}^2 \right) \right. \\
&+ \left(\gamma^2 + 4|\Omega_{23}|^2 + (\Delta\omega_{12} - \Delta\omega_{13})^2 \right) \times \\
&\left. \left(|\Omega_{23}|^4 + 2|\Omega_{23}|^2 (\gamma^2 - \Delta\omega_{12}\Delta\omega_{13}) + (\gamma^2 + \Delta\omega_{12}^2) (\gamma^2 + \Delta\omega_{13}^2) \right) \right. \\
&+ 2\Omega_{12}^2 \left(6|\Omega_{23}|^4 + 3\gamma^2 (\gamma^2 + \Delta\omega_{12}^2) + \Delta\omega_{12}\Delta\omega_{13} (\Delta\omega_{12}^2 - 3\gamma^2) + (3\gamma^2 + \Delta\omega_{12}^2) \Delta\omega_{13}^2 \right. \\
&\left. \left. - 4\Delta\omega_{12}\Delta\omega_{13}^3 + 2\Delta\omega_{13}^4 + |\Omega_{23}|^2 (9\gamma^2 + \Delta\omega_{12}^2 - \Delta\omega_{12}\Delta\omega_{13} + 10\Delta\omega_{13}^2) \right) \right] \tag{3}
\end{aligned}$$

which is rather formidable. Figure 1 displays plots of R_{ss} normalized by γ as a function of $\Delta\omega_{13}/\gamma$ calculated with $\Delta\omega_{12} = 1000\gamma$, $\Omega_{23} = \sqrt{2}\Omega_{12}$, and $\Omega_{12} = \gamma, 2\gamma \dots 20\gamma$. The assumption $\Omega_{23} = \sqrt{2}\Omega_{12}$ is the double harmonic oscillator approximation (DHOA) in the case where we have a two-photon excitation of a vibrational mode from the ground to the $\nu = 2$ state. If we take $|\Delta\omega_{12}| \gg |\Omega_{12}|, |\Omega_{23}| \gg \Delta\omega_{13}, \gamma$, and take the terms with the highest powers of $\Delta\omega_{12}$ in the numerator and denominator we get

$$R_{ss} = \frac{4\gamma|\Omega_{12}\Omega_{23}|^2}{\Delta\omega_{12}^2 (\gamma^2 + \Delta\omega_{13}^2) + (|\Omega_{12}|^2 + |\Omega_{23}|^2)^2} \tag{4}$$

The rate is centered on $\Delta\omega_{13} = 0$, with power broadened half-width, half maximum equal to $\gamma\sqrt{1 + ((|\Omega_{12}|^2 + |\Omega_{23}|^2)/\Delta\omega_{12}\gamma)^2}$. Neglecting the saturation correction, this is the same as was derived by Vasilenko *et al.*¹³.

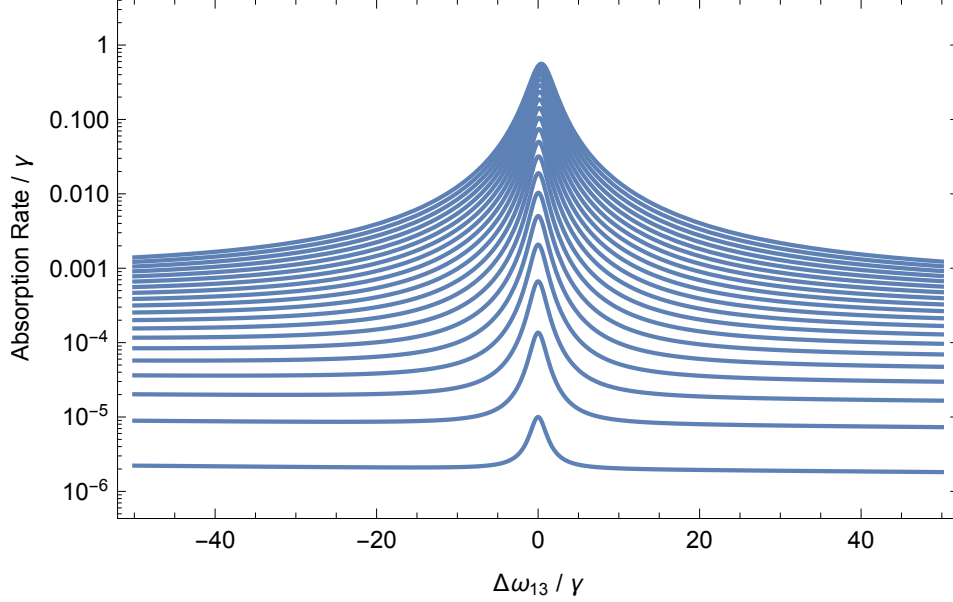


FIG. 1: Steady-State photon absorption rate as a function of detuning, $\Delta\omega_{12}$, from the two-photon resonance angular frequency, both normalized by γ , the relaxation rate. Calculations assumed that the detuning of the transition to the intermediate state (2) equals 1000γ , that the Rabi frequency for the second transition, $2 \rightarrow 3$ is $\sqrt{2}$ larger than Ω_{12} , the Rabi frequency for the $1 \rightarrow 2$, and that $\Omega_{12} = \gamma, 2\gamma, \dots, 20\gamma$.

If we drive exactly on the two-photon resonance $\Delta\omega_{13} = 0$, we can write R

$$R_{\text{SR}} = \frac{4\gamma|\Omega_{23}|^2|\Omega_{12}|^2\left(|\Omega_{12}|^2+|\Omega_{23}|^2+\gamma^2\right)}{\left(|\Omega_{12}|^2+|\Omega_{23}|^2\right)\left(\left(|\Omega_{12}|^2+|\Omega_{23}|^2+\gamma^2\right)^2+\gamma^2\Delta\omega_{12}^2\right)} - \frac{2\gamma\left(|\Omega_{23}|^2-|\Omega_{12}|^2\right)|\Omega_{12}|^2}{\left(|\Omega_{12}|^2+|\Omega_{23}|^2\right)\left(4\left(|\Omega_{12}|^2+|\Omega_{23}|^2\right)+\gamma^2+\Delta\omega_{12}^2\right)} \quad (5)$$

$$\xrightarrow{\Omega_{23}=\sqrt{2}\Omega_{12}} \frac{2}{3}\gamma|\Omega_{12}|^2\left(\frac{4\left(\gamma^2+3|\Omega_{12}|^2\right)}{\left(\gamma^2+3|\Omega_{12}|^2\right)^2+\gamma^2\Delta\omega_{12}^2}-\frac{1}{\gamma^2+12|\Omega_{12}|^2+\Delta\omega_{12}^2}\right) \quad (6)$$

which is the difference of two Lorentzians in $\Delta\omega_{12}$. Saturation of the two-photon transition becomes important at an intensity when $|\Omega_{12}|^2+|\Omega_{23}|^2 \sim |\Delta\omega_{12}|\gamma$. When $|\Delta\omega_{12}| \gg |\Omega_{12}|^2, |\Omega_{23}|^2 \gg |\Delta\omega_{12}|\gamma$, we have a saturation of the photon absorption rate $R_{\text{SR}} \rightarrow 4\gamma\left(\frac{|\Omega_{12}\Omega_{23}|}{|\Omega_{12}|^2+|\Omega_{23}|^2}\right)^2 \rightarrow (8/9)\gamma$ in the DHOA. This can be compared to a steady state absorption rate of γ if we assume that on hard saturation $\rho_{11} = \rho_{22} = \rho_{33} = 1/3$ or $\rho_{11} = \rho_{33} = 1/2, \rho_{22} = 0$.

We can expand R_{SR} in powers of Ω_{12} and Ω_{23} to obtain the absorption rate in powers of intensity

or photon number density. Keeping the terms up to fourth power in the Rabi frequencies, *i.e.* quadratic in light intensity, we have the low power limit as

$$R_{\text{SR}} = \frac{2\gamma\Omega_{12}^2}{\gamma^2 + \Delta\omega_{12}^2} - \frac{8\gamma\Omega_{12}^4}{(\gamma^2 + \Delta\omega_{12}^2)^2} + \frac{4\Omega_{23}^2\Omega_{12}^2}{\gamma(\gamma^2 + \Delta\omega_{12}^2)} + \dots \quad (7)$$

The first term on the right is the linear absorption from one-photon $1 \rightarrow 2$ absorption, the second the leading saturation term of that transition, and the last the two-photon absorption $1 \rightarrow 3$.

The above expressions should be applicable in the limit that $|\Delta\omega_{12}|$ is much larger than the Doppler width, in angular frequency units, for that transition. At resonance, we can use Eq. 6 to convolute the absorption rate with a normalized Gaussian Doppler broadening function to give a photon absorption rate per molecule in terms of the normalized Voigt lineshape function²¹ $g_V(\Delta\omega_{12}, \sigma_D, \gamma)$ where $\sigma_D^2 = k_B T_g \omega_{12}^2 / M c^2$ with T_g the translational temperature of the absorbers, and M their molecular mass. This gives a photon absorption rate:

$$R_{\text{SR}} = \frac{2\pi|\Omega_{12}|^2}{|\Omega_{12}|^2 + |\Omega_{23}|^2} \left(|\Omega_{23}|^2 g_V \left(\Delta\omega_{12}, \sigma_D, \frac{\gamma^2 + |\Omega_{12}|^2 + |\Omega_{23}|^2}{\gamma} \right) - \frac{\gamma(|\Omega_{23}|^2 - |\Omega_{12}|^2)}{\sqrt{\gamma^2 + 4|\Omega_{12}|^2 + 4|\Omega_{23}|^2}} g_V \left(\Delta\omega_{12}, \sigma_D, \sqrt{\gamma^2 + 4|\Omega_{12}|^2 + 4|\Omega_{23}|^2} \right) \right) \quad (8)$$

$$R_{\text{SR}} \xrightarrow{|\Omega_{23}|^2 = 2|\Omega_{12}|^2} \frac{8\pi|\Omega_{12}|^2}{3} g_V \left(\Delta\omega_{12}, \sigma_D, \frac{\gamma^2 + 3|\Omega_{12}|^2}{\gamma} \right) - \frac{2\pi\gamma|\Omega_{12}|^2}{3\sqrt{\gamma^2 + 12|\Omega_{12}|^2}} g_V \left(\Delta\omega_{12}, \sigma_D, \sqrt{\gamma^2 + 12|\Omega_{12}|^2} \right) \quad (9)$$

Note here, the second term is negative, canceling part of the contribution of the first term. Figure 2 displays the two-photon resonance photon absorption rate as a function of Rabi frequency for a range of values for the one-photon detuning, assuming the harmonic ratio $\sqrt{2}$ for the two Rabi frequencies. Figure 3 plots the photon excitation rate per molecule as a function of $\Delta\omega_{12}$, both normalized by γ and assuming a Doppler broadening parameter $\sigma_D = 100\gamma$. Curves are plotted (from bottom to top) for $\Omega_{12}^2 = \gamma^2, 2\gamma^2, \dots, 20\gamma^2$. The upper panel is the rate with both one and two-photon absorption, the lower where there is no two-photon absorption ($\Omega_{23} = 0$). Under the assumed parameters, even at exact one photon resonance, opening up the two-photon resonance increases the rate of photon absorption by nearly an order of magnitude. This is due to the fact that the one photon resonance is Doppler Broadened and the one photon excitation burns a whole in the ground velocity distribution, while the entire Doppler profile can absorb two-photons.

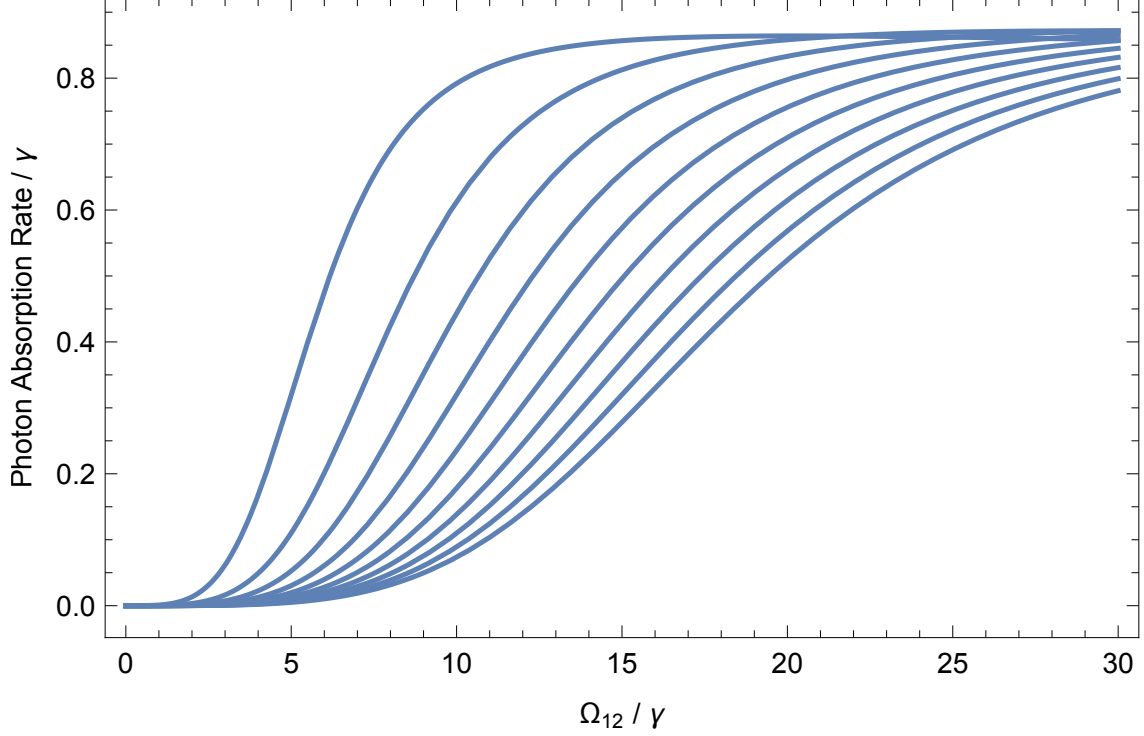


FIG. 2: Steady-State photon absorption rate at the two-photon resonance as a function of the pumping Rabi frequency, Ω_{12} , both normalized by γ , for several values of detuning of the one-photon transition. $\Omega_{23} = \sqrt{2}\Omega_{12}$ is assumed. The values of $\Delta\omega_{12} = 100\gamma, 200\gamma, \dots, 1000\gamma$ from left to right in the figure. The Doppler broadening of the one-photon absorption is assumed to be sufficiently smaller than the detuning so that it can be neglected.

If we convolute the Doppler broadening with the power series expansion for R_{SR} , Eq. 7, we get

$$\begin{aligned}
 R_{\text{SR}} = & 2\pi|\Omega_{12}|^2 \left(1 + 2\frac{|\Omega_{23}|^2 - |\Omega_{12}|^2}{\gamma^2} \right) g_{\text{V}}(\Delta\omega_{12}, \sigma_{\text{D}}, \gamma) \\
 & + \frac{4\pi|\Omega_{12}|^4}{\gamma} \left(\frac{\partial g_{\text{V}}(\Delta\omega_{12}, \sigma_{\text{D}}, \gamma)}{\partial \gamma} \right) + \dots
 \end{aligned} \tag{10}$$

If $|\Delta\omega_{12}|$ is large compared to σ_{D} , the sum of the two Ω_{12}^4 terms is smaller than the $\Omega_{12}^2\Omega_{23}^2$ term by a factor of $2(|\Omega_{12}|/\gamma/|\Omega_{23}|\Delta\omega_{12})^2 = (\gamma/\Delta\omega_{12})^2$ in the harmonic approximation, and thus will be negligible at low pressures.

II. INFLUENCE OF SPATIAL DEGENERACY

Up to this point, we have only considered three level systems without the spatial angular momentum projection degeneracy associated with levels with nonzero total angular momentum J , *i.e.*

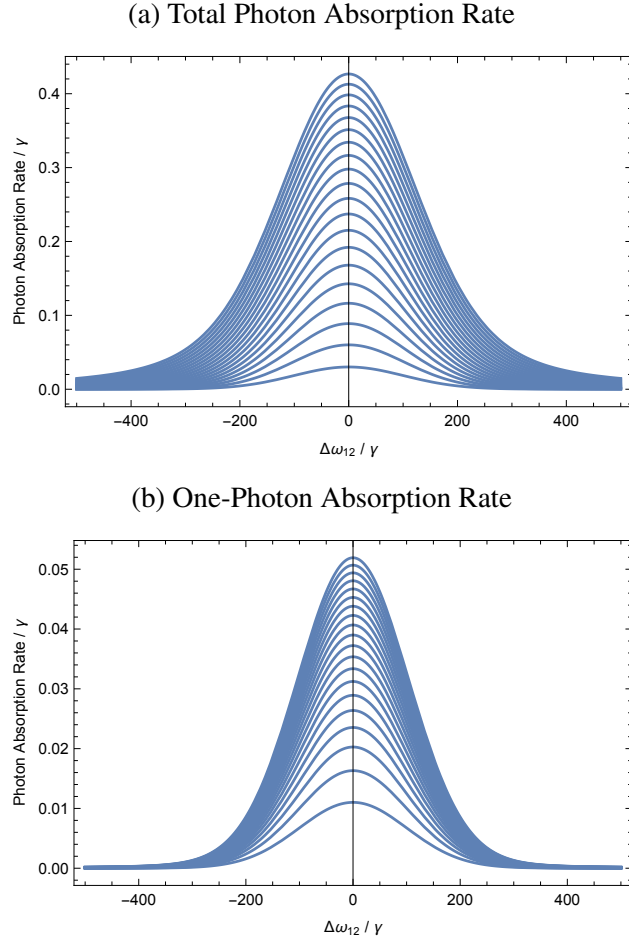


FIG. 3: a) Steady-State photon absorption rate at the two-photon resonance as a function of the one-photon detuning, $\Delta\omega_{12}$, normalized by γ . A Doppler broadening standard deviation of 100γ and $\Omega_{23} = \sqrt{2}\Omega_{12}$ are assumed. Curves are plotted as a function of $\Omega_{12}^2 = \gamma^2, 2\gamma^2, \dots, 20\gamma^2$, going from bottom to top. b) The Steady-State photon absorption rate with the same parameters except $\Omega_{23} = 0$, *i.e.* without the second transition.

the $2J + 1$ fold M degeneracy. For linear optical polarization, it is convenient to take the axis of angular momentum projection quantization parallel with the optical electric field, which results in optical absorption transitions having a $\Delta M = 0$ selection rule. For circular polarization, we take the axis of quantization along the direction of optical propagation, resulting in a $\Delta M = \pm 1$ selection rule for absorption from left or right handed polarized light respectively. The signs are flipped for stimulated emission. Linear absorption rates are independent of optical polarization state for an isotropic sample, which has equal initial population in each M state for any fixed set of values for the other quantum numbers. Two-photon absorption rates are different for linear and circular

polarization,²² though the same for right and left polarized radiation, so we will only consider polarization states (p) as linear (L) and circular (C) with the latter assumed to be right handed. Changes in TPA with polarization can be used to assign symmetries of the states involved.^{19,23}

Each of the Rabi frequencies will have a dependence on the M quantum numbers that can be represented as $\Omega_{i,j}(M_i, M_j) = \Omega_{i,j} \phi_p(J_i, M_i, J_j, M_j)$ where ϕ_p are the direction cosine matrix elements for polarization state p . The nonzero values are given in Table I.²⁴ The results presented above continue to hold if we replace Ω_{12} by $\Omega_{12} \phi_L(J_1, M, J_2, M)$ and Ω_{23} by $\Omega_{23} \phi_L(J_2, M, J_3, M)$ for linear polarization and by $\Omega_{12} \phi_C(J_1, M, J_2, M+1)$ and Ω_{23} by $\Omega_{23} \phi_C(J_2, M+1, J_3, M+2)$ for the case of circular polarization and then average the rate over the $2J_1 + 1$ initial values of M . Because the ϕ terms are different for the fundamental and overtone transitions, the simplification of the harmonic matrix element approximation no longer holds exactly.

For the photon absorption rate, neglecting saturation, we can replace the factor $\Omega_{12}^2 \Omega_{23}^2$ by

$$\Omega_{12}^2 \Omega_{23}^2 \rightarrow \frac{\Omega_{12}^2 \Omega_{23}^2}{2J_1 + 1} \sum_{M_1} \phi_p(J_1, M_1, J_2, M_2)^2 \phi_p(J_2, M_2, J_3, M_3)^2 \quad (11)$$

Using the line strength factor, S , Einstein spontaneous emission rate, $A_{i \rightarrow j}$, optical intensity, I , optical electric field amplitude, \mathcal{E} , transition frequency, ν ,

$$S_{ij} = 3 \langle v_i, J_i || \mu || v_j, J_j \rangle^2 \sum_{M_1, M_2} \phi_p(J_1, M_1, J_2, M_2)^2 = \frac{3\pi\epsilon_0 \hbar c^3 (2J_j + 1)}{\omega_{ij}^3} A_{i \leftarrow j} \quad (12)$$

$$\Omega_{ij}^2(J_1, M_1, J_2, M_2) = \frac{\mathcal{E}^2 \langle v_i, J_i || \mu || v_j, J_j \rangle^2}{4\hbar^2} \phi_p(J_1, M_1, J_2, M_2)^2 \quad (13)$$

Using $I = \epsilon_0 c |\mathcal{E}|^2 / 2 = h\nu N_p$, we can write the effective value for $\Omega_{12}^2 \Omega_{23}^2$ as

$$\Omega_{12}^2 \Omega_{23}^2 = \frac{\pi^2 c^4 I^2}{4\hbar^2 \omega^6} A_{1,2} A_{2,3} a_p(J_1, J_2, J_3) \quad (14)$$

$$a_L(J_1, J_2, J_3) = \frac{(2J_2 + 1)(2J_3 + 1)}{2J_1 + 1} \frac{\sum_M \phi_L(J_1, M, J_2, M)^2 \cdot \phi_L(J_2, M, J_3, M)^2}{\sum_M \phi_L(J_1, M, J_2, M)^2 \cdot \sum_M \phi_L(J_2, M, J_3, M)^2} \quad (15)$$

$$a_C(J_1, J_2, J_3) = \frac{(2J_2 + 1)(2J_3 + 1)}{2J_1 + 1} \frac{\sum_M \phi_C(J_1, M, J_2, M+1)^2 \cdot \phi_C(J_2, M+1, J_3, M+2)^2}{\sum_M \phi_C(J_1, M, J_2, M+1)^2 \cdot \sum_M \phi_C(J_2, M, J_3, M+1)^2}$$

The dimensionless factors $a_p(J_1, J_2, J_3)$ account to the spatial degeneracy. Their nonzero values are given in Table II. All the a_p factors are on the order of unity, but some two-photon transitions are favored by linear polarization (RR, RP, PR, PP, QQ) and some by circular polarization (QR, QP, RQ, PQ). For the $P(J) - R(J-1)$ sequence, linear polarization produces four times the excitation rate as circular polarization.

TABLE I: Direction Cosine Matrix Element Factors²⁴

	$J' = J-1$	$J' = J$	$J' = J+1$
$\phi_L(J, M, J', M)$	$\frac{\sqrt{J^2 - M^2}}{(J^2(4J^2 - 1))^{1/4}}$	$\frac{M}{\sqrt{J(J+1)}}$	$\frac{\sqrt{(J+1)^2 - M^2}}{((J+1)^2(2J+1)(2J+3))^{1/4}}$
$\phi_C(J, M, J', M+1)$	$\frac{\sqrt{(J-M)(J-M-1)}}{(4J^2(4J^2 - 1))^{1/4}}$	$\frac{\sqrt{(J-M)(J+M+1)}}{\sqrt{2J(J+1)}}$	$-\frac{\sqrt{(J+M+1)J+M+2}}{(4(J+1)^2(2J+1)(2J+3))^{1/4}}$

 TABLE II: a_p factors to correct for M dependence in off resonance two-photon excitation rate

J_2	J_3	$a_L(J_1, J_2, J_3)$	$a_C(J_1, J_2, J_3)$	a_L high J	a_C high J
$J_1 + 1$	$J_1 + 2$	$\frac{6(2J_1+5)}{5(2J_1+1)}$	$\frac{9(2J_1+5)}{5(2J_1+1)}$	6/5	9/5
$J_1 + 1$	$J_1 + 1$	$\frac{3J_1(2J_1+3)}{5(J_1+1)(2J_1+1)}$	$\frac{9J_1(2J_1+3)}{10(J_1+1)(2J_1+1)}$	3/5	9/10
$J_1 > 0$	$J_1 + 1$	$\frac{3(J_1+2)(2J_1+3)}{5(J_1+1)(2J_1+1)}$	$\frac{9(J_1+2)(2J_1+3)}{10(J_1+1)(2J_1+1)}$	3/5	9/10
$J_1 + 1$	J_1	$\frac{3(4J_1^2+8J_1+5)}{5(J_1+1)(2J_1+1)}$	$\frac{3J_1(2J_1-1)}{10(J_1+1)(2J_1+1)}$	6/5	3/10
J_1	J_1	$\frac{3(3J_1^2+3J_1-1)}{5J_1(J_1+1)}$	$\frac{3(2J_1+3)(2J_1-1)}{10J_1(J_1+1)}$	9/5	6/5
$J_1 - 1$	$J_1 > 0$	$\frac{3(4J_1^2+1)}{5J_1(2J_1+1)}$	$\frac{3(J_1+1)(2J_1+3)}{10J_1(2J_1+1)}$	6/5	3/10
$J_1 > 0$	$J_1 - 1 > 0$	$\frac{3(J_1-1)(2J_1-1)}{5J_1(2J_1+1)}$	$\frac{9(J_1-1)(2J_1-1)}{10J_1(2J_1+1)}$	3/5	9/10
$J_1 - 1 > 0$	$J_1 - 1$	$\frac{3(J_1+1)(2J_1-1)}{5J_1(2J_1+1)}$	$\frac{9(J_1+1)(2J_1-1)}{10J_1(2J_1+1)}$	3/5	9/10
$J_1 - 1 > 0$	$J_1 - 2$	$\frac{6(2J_1-3)}{5(2J_1+1)}$	$\frac{9(2J_1-3)}{5(2J_1+1)}$	6/5	9/5

Keeping the $\Omega_{12}^2 \Omega_{23}^2$ term in Eq 7, and using Eq. 14 for the effective value, we have for the on two-photon resonance steady state absorption rate

$$R_{\text{SR}} = \frac{4\Omega_{12}^2 \Omega_{23}^2}{\gamma(\gamma^2 + \Delta\omega_{12}^2)} = \frac{\pi^2 c^4}{\hbar^2 \omega^6 \gamma (\gamma^2 + \Delta\omega_{12}^2)} I^2 A_{1,2} A_{2,3} a_p(J_1, J_2, J_3) \quad (16)$$

It has been assumed that ω_{12} and ω_{23} can be replaced the two-photon angular frequency, $\omega = (\omega_{12} + \omega_{23})/2$.

Averaging over the Doppler Broadening of $\Delta\omega_{12}$ gives

$$R_{\text{SR}} = \frac{\pi^3 c^4}{\hbar^2 \omega^6 \gamma^2} g_V(\Delta\omega_{12}, \sigma_D, \gamma) A_{1,2} A_{2,3} a_p(J_1, J_2, J_3) I^2 \quad (17)$$

$$= \frac{\pi^3 c^4}{\omega^4 \gamma^2} g_V(\Delta\omega_{12}, \sigma_D, \gamma) A_{1,2} A_{2,3} a_p(J_1, J_2, J_3) N_p^2 \quad (18)$$

where N_p is the photon flux rate. Converting molecular parameters, except the $A_{i \rightarrow j}$ values, to dimensions of cm^{-1} , as that is how spectroscopic parameters are usually tabulated, we have

$$R_{\text{SR}} = \frac{1}{64\pi^4 h^2 c^5 \tilde{\nu}^6 \Delta\tilde{\nu}_{\text{H}}^2} g_{\text{V}}(\Delta\tilde{\nu}_{12}, \tilde{\sigma}_{\text{D}}, \Delta\tilde{\nu}_{\text{H}}) A_{1,2} A_{2,3} a_p(J_1, J_2, J_3) I^2 \quad (19)$$

$$= \sigma_{13}^{(2)} N_{\text{p}}^2 = \frac{1}{64\pi^4 c^3 \tilde{\nu}^4 \Delta\tilde{\nu}_{\text{H}}^2} g_{\text{V}}(\Delta\tilde{\nu}_{12}, \tilde{\sigma}_{\text{D}}, \Delta\tilde{\nu}_{\text{H}}) A_{1,2} A_{2,3} a_p(J_1, J_2, J_3) N_{\text{p}}^2 \quad (20)$$

The homogeneous broadening wavenumber can be calculated as $\Delta\tilde{\nu}_{\text{H}} = \gamma/2\pi c = b_p P_{\text{g}}$ where b_p is the pressure broadening coefficient (half width at half maximum, HWHM) and P_{g} the pressure of the gas sample. The above results are rates and cross sections per molecules in state 1. For reference to the molecules of a specific compound in the gas, we should multiply by the fraction of those molecules in state 1, $f_1 = g_1 \exp(-hcT_1/k_{\text{B}}T_{\text{g}})/Q(T_{\text{g}})$, where g_1 , and T_1 , are the degeneracy and term value (energy converted to cm^{-1}) of state 1 respectively and $Q(T_{\text{g}})$ is the partition function for that molecule. If $|\Delta\tilde{\nu}_{12}| \gg \tilde{\sigma}_{\text{D}}$ and $\Delta\tilde{\nu}_{\text{H}}$, then $g_{\text{V}} \rightarrow \Delta\tilde{\nu}_{\text{H}}/(\pi\Delta\tilde{\nu}_{12}^2)$. If $\tilde{\sigma}_{\text{D}} \gg |\Delta\tilde{\nu}_{12}|$ and $\Delta\tilde{\nu}_{\text{H}}$, *i.e.* there is exact double resonance for a frequency near the center of the Doppler lineshape, then $g_{\text{V}} \rightarrow 1/\sqrt{2\pi}\tilde{\sigma}_{\text{D}}$.

Based upon Eqs. 4 and 14, it can be shown that, in the off-resonance case ($\Delta\tilde{\nu}_{12} \gg \tilde{\sigma}_{\text{D}}, |\Omega_{12}|, |\Omega_{23}|$ and γ), optical saturation will reduce the on-resonance two-photon absorption by a factor of $\sqrt{1 + (I/I_{\text{sat}})^2}$ where we can write:

$$I_{\text{sat}} = \frac{64\pi^4 \hbar c^3 \Delta\tilde{\nu}_{12} \Delta\tilde{\nu}_{\text{H}} \Delta\tilde{\nu}^3}{(A_{12} + A_{23}) \sqrt{a_{\text{p}}}} \quad (21)$$

Note that the saturation power scales linearly with $\Delta\tilde{\nu}_{\text{H}}$ and thus pressure, unlike for a Doppler Broadened line where the saturation power scales as the square of $\Delta\tilde{\nu}_{\text{H}}$ and thus pressure squared. Also, for high power, $I \gg I_{\text{sat}}$, the absorption signal.

III. CAVITY RING-DOWN DETECTION OF TWO-PHOTON ABSORPTION

We will relate the steady state two-photon absorption rate to the rate of decay of intra-cavity intensity. Let the number density of molecules in state 1 at equilibrium be N_1 and assume the molecules are excited by the TEM_{00} of a confocal cavity with one way intra-cavity power P_{ic} . If the cavity intensity decay rate and the transit rate of molecules across the cavity mode are slow compared to γ , we can assume that molecular absorption remains in steady state with the instantaneous intensity at the position of each molecule. The rate at which optical energy is absorbed from the intra-cavity field will equal the integral of $hc\tilde{\nu}R_{\text{ss}}N_1$ over the cavity. Assuming the cavity

is nearly confocal with length L , the integral of I^2 over the cavity volume gives $(3/2)\pi\tilde{\nu}P_{\text{ic}}^2$.²⁵ Neglecting saturation, the power absorbed by the molecules inside the cavity is given by:

$$P_{\text{abs}} = \frac{g_{\text{V}}(\Delta\tilde{\nu}_{12}, \tilde{\sigma}_{\text{D}}, \Delta\tilde{\nu}_{\text{H}})A_{12}A_{23}a_p(J_1, J_2, J_3)N_1f_1}{128\pi^3hc^4\tilde{\nu}^4(\Delta\tilde{\nu}_{\text{H}}^2 + \Delta\tilde{\nu}_{13}^2)}P_{\text{ic}}^2 \quad (22)$$

Note this is independent of the cavity length due to the fact that a shorter cavity has a more tightly focused mode. The optical energy stored in the cavity equals $(2L/c)P_{\text{ic}}$, so $dP_{\text{ic}}/dt = -(c/2L)P_{\text{abs}}$.

Consider on resonance excitation on the TPA ($\Delta\tilde{\nu}_{13} = 0$), and an ideal gas at pressure and temperature, P_g, T_g , for which $\Delta\tilde{\nu}_{\text{H}} = b_pP_g$ and $N_1 = (P_g/k_{\text{B}}T_g)x_a$ where x_a is the mole fraction of the analyte in the sample gas. These assumptions lead to a rate of loss of intra-cavity power

$$\frac{dP_{\text{ic}}}{dt} = -\gamma_1P_{\text{ic}} - \gamma_2P_{\text{ic}}^2 \quad (23)$$

$$\gamma_1 = c \left(\alpha + \frac{1 - R_{\text{m}}}{L} \right) \quad (24)$$

$$\gamma_2 = \frac{g_{\text{V}}(\Delta\tilde{\nu}_{12}, \tilde{\sigma}_{\text{D}}, b_pP)A_{12}A_{23}a_p(J_1, J_2, J_3)x_af_1}{256\pi^3hc^3Lk_{\text{B}}T_g\tilde{\nu}^4b_p^2P_g} \quad (25)$$

$$\gamma_2 \xrightarrow{|\Delta\tilde{\nu}_{12}| \gg \tilde{\sigma}_{\text{D}}, b_pP} \frac{A_{12}A_{23}a_p(J_1, J_2, J_3)x_af_1}{256\pi^4hc^3Lk_{\text{B}}T_g\Delta\tilde{\nu}_{12}^2\tilde{\nu}^4b_p} \quad (26)$$

which can be integrated to give the Power vs. time

$$P_{\text{ic}}(t) = \frac{\gamma_1P_{\text{ic}}(0)\exp(-\gamma_1t)}{\gamma_1 + \gamma_2P_{\text{ic}}(0)(1 - \exp(-\gamma_1t))} \quad (27)$$

Above, α denotes the linear absorption coefficient of the intracavity sample, including the one photon $1 \rightarrow 2$ transition, and R_{m} is the geometric mean of the power reflectivity of the two cavity mirrors. Note that for a detuning that is large compared to the Doppler width, the two-photon absorption rate is independent of pressure. This will breakdown if the pressure is so low that either saturation or transit time broadening of the TPA cannot be ignored. When the intermediate state detuning is well within the Doppler broadening, the two-photon absorption rate is inversely proportional to gas pressure.

In the expressions above, I have only considered the Doppler-Free absorption from the counter propagating waves in the cavity. There is also a Doppler Broadened term as well, with the same width as for a one-photon transition at the same frequency. The average of the intracavity intensity squared along the beam gives $6I^2$ while each traveling wave interacts separately for the Doppler broadened absorption giving a factor of I^2 for each direction, so the ratio Doppler broadened to Doppler-free absorption is given in terms of the normalized lineshape functions $3g_{\text{D}}(\nu)/g_{\text{L}}(\nu)$

which on resonance equals $\sqrt{\ln(2)/9\pi}(\Delta\nu_H)/\Delta\nu_D = 0.1565(\Delta\nu_H/\Delta\nu_D)$. The half-width values should both be either full width at half maximum (FWHM) or HWHM values. As Doppler-free absorption will saturate at pressures where $\Delta\nu_H \gg \Delta\nu_D$, the Doppler broadening contribution will likely be negligible.

IV. APPLICATION TO CARBON DIOXIDE AND OTHER MOLECULES

Consider a parallel two-photon transition of a linear molecule with a Σ ground state $\nu_s = 0 \rightarrow 1 \rightarrow 2$. There will be $S(J)(\Delta J = 2)$, $Q(J)(\Delta J = 0)$ and $O(J)(\Delta J = -2)$ transitions, with the largest resonance enhancement for one of the Q branch transitions. As the $\nu = 1 \rightarrow 2$ ‘‘hot band’’ is typically red shifted from the $\nu = 0 \rightarrow 1$ fundamental, the resonance will be largest for the J values near where the $P(J)$ branch of the fundamental crosses the $R(J - 1)$ branch of the hot band. Neglecting centrifugal distortion and higher order vibration-rotation interaction constants, the nearest resonant two-photon transitions will be $Q(J)$ transitions will have detuning given by:

$$\Delta\nu_{12}(\nu_s = 0, J \rightarrow \nu_s = 1, J - 1 \rightarrow \nu_s = 2, J) = -X_{ss} + 2(B_0 - \alpha_s)J \quad (28)$$

X_{ss} is the anharmonicity constant of mode s , B_0 the ground vibrational state rotational constant, and α_s the vibration-rotation interaction constant for mode s . Typical values for the X_{ss} constants are -5 to -50 cm^{-1} . The transition with the smallest $|\Delta\nu_{12}|$ occurs for the integer J value closest to $-X_{ss}/2(B_0 - \alpha_s)$ and this J value has a detuning less than $B_0 - \alpha_s$, except in the cases of J states with zero nuclear spin weight. If the ground state is not Σ symmetry, we also have additional near resonant transitions $J \rightarrow J - 1 \rightarrow J - 1$ and $J \rightarrow J \rightarrow J + 1$ with detuning of $X_{ss} + B_0J$ and $X_{ss} + (B_0 - 2\alpha_s)(J + 1)$ respectively. While we can expect, on average, the closest of these to be even closer to two-photon resonance, the Q branch transitions of parallel bands are weak, so these are unlikely to be the strongest unless they are particularly near resonant.

For perpendicular modes of such a linear molecule, t , we have possible transitions from the ground state to the $2\nu_t, \Sigma(l = 0)$ and $\Delta(l = \pm 2)$ vibrational states. For the Σ state, there will be near resonances again for the $J \rightarrow J - 1 \rightarrow J$ transition, but with detuning given by $X_{tt} - g_{tt}/2 + 2(B_0 - \alpha_t - q_t)J$. For the transitions to the Δ state, the $J \rightarrow J - 1 \rightarrow J$ excitation path has detuning $X_{tt} + g_{tt}/2 + 2(B_0 - \alpha_t - q_t/2)J$. In addition, there are near resonant transitions with excitation paths $J \rightarrow J - 1 \rightarrow J - 1$ and $J \rightarrow J \rightarrow J + 1$. These have detuning of $X_{tt} + g_{tt}/2 + (B_0 - q_t/2)J$ and $X_{tt} + (B_0 - 2\alpha_t + q_t)/2(J + 1)$. Unlike the case of the parallel transitions, the Q branch transitions

are strong, and the closest resonance of these will have a detuning less than $\sim B_0/2$.

As a quantitative example, we consider two-photon absorption by $^{12}\text{C}^{16}\text{O}_2$ gas in the region of the ν_3 fundamental. Transitions for both the fundamental and hot band in this mode are listed in the HITRAN database²⁶, which gives the parameters needed to calculate the two-photon cross section. ν_3 is the antisymmetric stretching mode, well known to be extremely intense with $A_{01} = 215.4/\text{s}$, $A_{12} = 401/\text{s}$. $X_{33} = -12.63 \text{ cm}^{-1}$ in this case. The nearest resonant two-photon transition is $Q(16)$ at $\tilde{\nu} = 2335.826 \text{ cm}^{-1}$, which is the mean of the transition wavenumber for the $P(16)$ of the fundamental band and $R(15)$ of the fundamental to overtone band. The $P(16)$ transition of the fundamental band off-resonance by only 0.093 cm^{-1} (2.8 GHz). The other intermediate state transitions that contributes to the two-photon amplitude is the $R(16)$ of the fundamental and $P(17)$ of the fundamental to overtone band. That is off-resonance by $\sim 66B \sim 25.7 \text{ cm}^{-1}$ with nearly the same dipole matrix elements and thus makes a negligible contribution to the two-photon absorption. The air broadening coefficients of each transition is listed as $b_p = 0.076 \text{ cm}^{-1}/\text{atm}$. At a gas temperature $T_g = 300 \text{ K}$, $J=16$ is near to the Boltzmann maximum with fractional population $f_1 = 0.075$ and the Doppler width parameter $\Delta\tilde{\omega}_D = 0.00186 \text{ cm}^{-1}$ (56 MHz). For this transition, $a(J_0, J_1, J_2) = 1.165$. At 1 torr total pressure, a two-photon cross section of $7.48 \cdot 10^{-39} \text{ cm}^4\text{s}$ per CO_2 molecule in the $J = 16$ state or $5.61 \cdot 10^{-40} \text{ cm}^4\text{s}$ per CO_2 molecule is calculated from these parameters using Eq. 20. This can be compared to a “typical” two-photon cross section for electronic transitions, which are measured in units of $10^{-50} \text{ cm}^4\text{s}$, which is known as one Göppert-Mayer (GM).¹⁹ For example, Squaraine Fluorophores, developed to be “Ultra-Bright” for two-photon microscopy²⁷ have peak two-photon excitation cross sections on the order of 10^4 GM, *i.e.* $10^{-46} \text{ cm}^4\text{s}$, 7 orders of magnitude smaller than for the resonantly enhanced transition in CO_2 .

For the signal estimate, we will take the parameters for the cavity used by Gali *et al.* in their $^{14}\text{CO}_2$ SCARS measurements:⁹ $L = 1 \text{ m}$, $T_M = 87 \text{ ppm}$, $1 - R_M = 190 \text{ ppm}$, which imply $\gamma_1 = 5.7 \cdot 10^4/\text{s}$, neglecting any linear loss from the sample. For mode-matched, monochromatic excitation of such a cavity, the predicted peak transmission is $(T_M/(1 - R_M))^2 = 0.21$. Assuming, like them, we use a laser with 100 mW power to excite the cavity, the predicted output power is $P_0 = 21 \text{ mW}$; an initial intracavity power $P_{ic}(0) = 241 \text{ W}$ each way. For such parameters, $\gamma_2 = 2.12 \cdot 10^8 x(\text{CO}_2)/(\text{W s})$ is calculated. Previously, I published an error propagation calculation that predicted the standard error of the parameters for fits to the two-photon loss decay transient given by Eq. 27.¹² For the case of shot-noise-limited detection, the standard error for γ_2 from a

single decay can be written as:

$$\sigma'(\gamma_2) = \frac{1}{P_{ic}(0)} \sqrt{\frac{6hc\tilde{\nu}}{Q_{det}P_{det}}} \gamma_1^{3/2} \quad (29)$$

Taking a detector quantum efficiency $Q_{det} = 0.63$ and power on the detector as $P_{det} = 10$ mW, and $\gamma_1 = 5.69 \cdot 10^4$ /s, gives $\sigma'(\gamma_2) = 2.6 \cdot 10^{-4}$ /W s. Assuming cavity decays were detected at a rate of 3 kHz ($\sim \gamma_1/20$), we get a detection noise equivalent γ_2 of $5.1 \cdot 10^{-6}$ / W s $\sqrt{\text{Hz}}$. Comparing this to the calculated value of γ_2 as a function of $x(\text{CO}_2)$ gives a predicted sensitivity of $x(\text{CO}_2) = 22$ ppq (10^{-15}) $\text{Hz}^{-1/2}$. This sensitivity value can be compared to the sensitivity limit of 5 ppq in 2 hr integration for $^{14}\text{C}^{16}\text{O}_2$ reported by Galli *et al.*⁹ using the SCAR technique¹¹ and a cavity cell cooled to 170 K, which translates to a sensitivity of 425 ppq per $\sqrt{\text{Hz}}$.

The selectivity of two-photon absorption is illustrated by looking at the relative strength of the different two-photon transitions in the ν_3 fundamental region. Figure 4 displays a comparison on the calculated $^{12}\text{C}^{16}\text{O}_2$ ν_3 and $2\nu_3$ relative intensities for the different rotational transitions, normalized such that the sum of intensities for both one-photon (P and R branches), and the two-photon (O, Q, S branches) transitions equals unity. Calculations used a 300 K rotational temperature. The $Q(16)$ transition is 250 times stronger than the next most intense transitions ($Q(14)$ and $Q(18)$) and about 1000 times stronger than the strongest lines in the O ($\Delta J = -2$) and S ($\Delta J = +2$) branches. We can expect qualitatively similar behavior in the TPA spectrum of most molecules that could be potential interferences in the detection of other analytes.

The author has searched the HITRAN online²⁸ database for a number of molecules for two-photon transitions where the fundamental and overtone level are listed, the later by either the corresponding hot band or by an overtone band from the ground state. In the former, A values are listed for both transitions that make up a resonant TPA triplet of states and these were used to calculate the TPA cross section of each transition. In the latter case, the A value for the $\nu = 1 \rightarrow 2$ transition was assumed to equal twice that of the fundamental, in accord with the double harmonic oscillator approximation. The strongest transitions for each isotopic species are given in Supplementary material to this paper.

We will now consider application of TPA to a relatively heavy asymmetric top molecule, which has much more complex level structure than CO_2 . For a molecule without symmetry, most ground vibrational state rotational levels will have 25 two-photon absorption transitions for each final vibrational level¹⁹ (O, P, Q, R, S branches for both ΔJ and ΔK), even without considering transitions allowed by asymmetry mixing that gives intensity to $|\Delta K_{a,c}| > 1$ transitions. While sensitivity re-

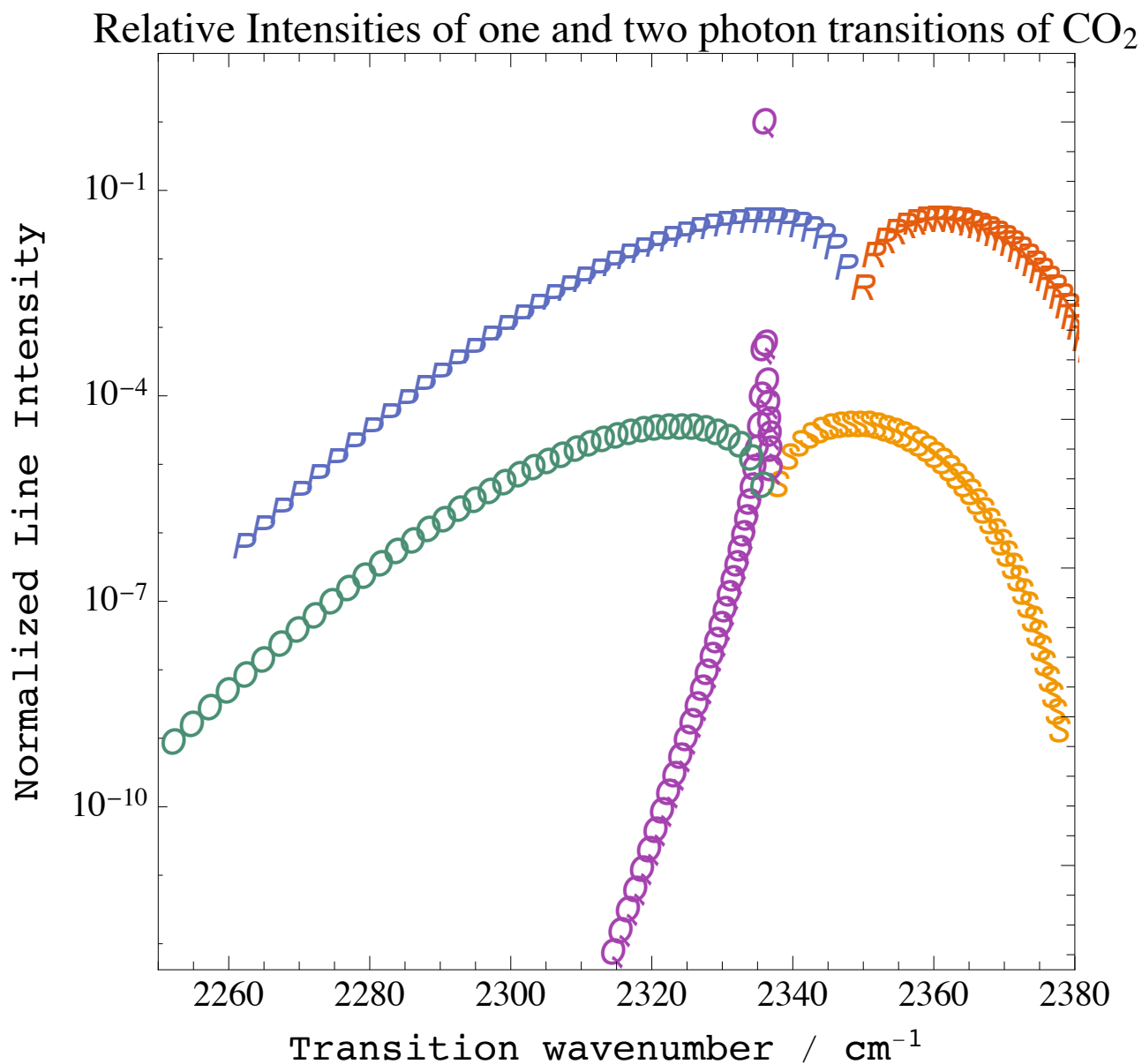


FIG. 4: Comparison of relative intensities of one and two-photon transitions of ¹²C¹⁶O₂. Type of transition is indicated by letter with O, P, Q, R, S representing $\Delta J = -2, -1, 0, 1, 2$. The one and two-photon bands are each normalized to have unity integrated intensity for the band

mains important, a more frequent limitation in the detection of these molecules, particularly using IR spectroscopy, is the difficulty in selectively detecting one species from another, particularly if they contain the same generic IR “functional groups”. As an example, I have calculated the two-photon absorption spectrum of trans-Butadiene (t-BD), point group C_{2h} , using anharmonic spectroscopic constants calculated from Quantum Chemistry;²⁹ kindly supplied to me by Dr. Manik

Pradhan. Calculations were done using Gaussian-16, with the 6-311++g(3df,2p) basis set and the B3YLP functional. Table III contains the calculated spectroscopic constants for the fundamentals and first overtone for each of the IR active normal modes of t-BD. The predicted constants explicitly include near resonant Fermi and Darling Dennison resonances. Normal modes numbered 10-13 are A_u symmetry representations and give C-axis polarized IR fundamentals. Modes numbered 17-24 are B_u representations and have mixed A,B-polarized IR fundamentals. I did not have the relative contributions of the A and B axis transition dipole matrix elements, so I took them to be equal. Calculations were done in the rigid rotor approximation, including all transitions with total angular momentum quantum number, J , up to 100. At 300 K, t-BD has a rotational partition function of 32 037. For fundamental bands, the strongest individual transitions having fractional intensities of 6.29, 4.83, 3.04, and 9.47×10^{-4} of the entire IR band for A, B, A/B hybrid, and C polarized bands, respectively, where the hybrid band is assumed to have equal A and B contributions. One way to characterize an effective number of transitions is by the ratio $(\sum I_t)^2 / \sum I_t^2$ where I_t is the absorption intensity of the t -th transition. Neglecting the frequency factors in the intensities, this effective number of transitions is calculated as 3410, 7380, 9549, and 6420 for the A, B, A/B hybrid, and C polarized bands.

The two-photon absorption spectrum of t-BD from the ground vibrational state to the two quanta level in each of the the IR allowed modes was calculated using Eq. 1 for the two-photon amplitude and expressing the intensity as proportional to the square magnitude of the transition amplitude times the lower state population. The sum over intermediate states included all allowed transitions in the fundamental level. In order to approximately account for Doppler broadening of intermediate state resonances, the Doppler width was treated as homogeneous broadening, i.e. $\gamma = 2\pi c \Delta\nu_D$ in Eq. 1 where $\Delta\nu_D$ is the Doppler half width, half maximum. 300 K thermal populations were assumed for the ground vibrational state and thermal population of the excited vibrational states was neglected. Intensities of each two-photon transition were initially calculated using only the direction cosine matrix elements to allow comparison of different normal modes without the complication of their different IR intensity values, giving transition intensities in units of cm^2 . The results of these calculations are summarized in Table IV. The total intensity, summed over all TPA transitions is given in the table, and is found to vary widely with normal mode, spanning the range from 30 - 11,000 cm^2 . The differences are due to the small differences in upper state rotational constants and the different values for the diagonal anharmonicity calculated from the $\nu = 0 \rightarrow 1$ and $\nu = 1 \rightarrow 2$ vibrational intervals. The effective number of transitions, as de-

fined above for the fundamentals, varies between a low of 2.74 to a high of 67, indicating even for this largest values, that the TPA spectrum is dramatically sparser than the fundamentals. Another way to characterize how sparse the TPA spectra are is by the fraction of total intensity carried by the strongest transition in the band. These vary from a low of 0.053 to a high of 0.59, i.e. 59% of the total band intensity is contained in a single transition. The rotational quantum numbers for the strongest transitions of each band are listed and are distinct in each case, reflecting the fact that the strongest transitions are extremely sensitive to the constants of the three vibrational states involved. Also listed is the two-photon cross section for each of the strongest transitions (integrated over transition wavenumber) to give units of $\text{cm}^3 \text{ s}$. Given the high sensitivity to spectroscopic constants, the presently presented calculations are unlikely to be quantitatively accurate, but they should be considered representative of the expected size of these quantities, at laboratory temperatures, for a molecule of the size of t-BD.

In many applications of Cavity ring-down and other forms of Cavity Enhanced Spectroscopy, the ultimate sensitivity limit is determined by drifts in the empty cavity loss. By scanning the laser over a resonant absorption or by frequency jumping on and off resonance, cavity loss drift that changes slowly with wavelength relative to the absorption line-width are corrected for, but there remain “fringes” that arise from interferences. These can arise from scattering by any of the optics that couple back into the resonator. Scattering of a single photon back into the cavity during the decay will just be detectable when the decay is shot-noise limited.³⁰ These interference fringes often have widths comparable with Doppler Broadened lines. For the CO_2 fundamental, the Doppler FWHM is ~ 130 MHz, similar to the FSR of an interference caused by a back reflection from an optic 1 m from a cavity mirror (150 MHz). At total gas pressure on the order of 1 torr, the TPA line-width will typically be on the order of a few MHz, which is far narrower than any fringe produced by feedback. Galli *et. al.*^{9,11} have demonstrated that the SCARS method (where the molecular absorption is saturated and thus changes during the cavity decay) allows a separation of the molecular loss from all the contributions to the empty cavity loss; only the latter is effected by the instability cause by interference. This is what allows them to improve their sensitivity limit by very long time integration. This feature has also been theoretically demonstrated for TPA, with reduced correlation of the fitted linear and TPA loss rates compared to the saturable and non-saturable loss rates that are fitting parameters in the SCARS technique.¹²

In order that the TPA not be strongly saturated, one needs to select the intracavity pressure such that the excitation rate per resonant molecule is less than the relaxation rate, which is proportional

TABLE III: Calculated Spectroscopic constants for trans-Butadiene vibrational states

state	Sym	G(v) cm ⁻¹	Intensity km/mol.	A cm ⁻¹	B cm ⁻¹	C cm ⁻¹
G.S.	Ag	0		1.3980866	0.1476468	0.1334412
v(10)	Au	1029.019	22.44	1.394038	0.148405	0.133465
v(11)	Au	927.810	79.63	1.36601	0.147538	0.133479
v(12)	Au	530.252	11.53	1.394707	0.147527	0.13344
v(13)	Au	168.965	0.60	1.338177	0.147815	0.133823
v(17)	Bu	3080.483	25.42	1.395197	0.147566	0.133357
v(18)	Bu	2998.877	3.87	1.39411	0.147563	0.133341
v(19)	Bu	2977.928	22.46	1.394491	0.147568	0.133342
v(20)	Bu	1614.113	26.66	1.395653	0.147366	0.133123
v(21)	Bu	1388.271	4.33	1.400366	0.147668	0.133366
v(22)	Bu	1303.287	0.68	1.403727	0.147775	0.133385
v(23)	Bu	995.753	1.81	1.424255	0.146821	0.13336
v(24)	Bu	303.799	2.75	1.45607	0.147641	0.133369
		G(v) cm ⁻¹	X(s,s) cm ⁻¹	A cm ⁻¹	B cm ⁻¹	C cm ⁻¹
2v(10)	Ag	2054.497	-3.541	1.38999	0.149162	0.133491
2v(11)	Ag	1857.59	1.97	1.333933	0.147428	0.133519
2v(12)	Ag	1058.985	-1.519	1.391328	0.147407	0.133439
2v(13)	Ag	336.738	-1.192	1.278268	0.147982	0.134205
2v(17)	Ag	6159.571	-1.395	1.392308	0.147483	0.133274
2v(18)	Ag	5999.975	2.221	1.390133	0.147479	0.133242
2v(19)	Ag	5995.06	39.204	1.390896	0.147488	0.133244
2v(20)	Ag	3226.105	-2.121	1.39322	0.147083	0.132806
2v(21)	Ag	2773.766	-2.776	1.402646	0.147687	0.133292
2v(22)	Ag	2596.266	-10.308	1.409368	0.147901	0.13333
2v(23)	Ag	1992.229	0.723	1.450423	0.145993	0.13328
2v(24)	Ag	609.207	1.609	1.514054	0.147635	0.133299

TABLE IV: Calculated Two-Photon IR absorption of trans-Butadiene overtone of each IR allowed mode

mode	$\Delta\nu_D$ MHz	total Int. cm ²	N eff	I max / I tot	ν cm ⁻¹	$\int \sigma^2$ cm ³ sec	Transition	E'' cm ⁻¹
10	18.9	146.8	10.49	0.1818	1019.9716	1.47819E-43	26(4, 22) → 26(2, 24)	118.8634
11	17.1	205	2.79	0.5883	933.535	1.19819E-41	35(3, 32) → 36(3, 44)	190.0674
12	9.8	372.9	2.75	0.4522	541.9089	3.09595E-42	21(1, 21) → 23(3, 21)	64.3248
13	3.1	1.10E04	8.864	0.1913	154.7277	1.59542E-41	14(7, 8) → 14(5, 10)	91.1398
17	56.6	52.96	14.91	0.1442	3074.0817	6.57796E-46	18(3, 16) → 17(2, 16)	59.4442
18	55.1	31.1	17.33	0.1331	2995.6409	9.19439E-48	20(1, 19) → 19(0, 19)	61.5281
19	54.7	30.26	36.18	0.0721	2986.1806	1.64691E-46	26(13, 14) → 27(12, 16)	311.2058
20	29.7	97.43	7.754	0.293	1604.6385	3.64311E-44	35(3, 33) → 34(2, 33)	188.7359
21	25.5	214.63	67.13	0.0529	1391.7118	6.7642E-46	10(3, 7) → 10(3, 7)	17.0934
22	23.9	70.17	7.33	0.2747	1297.9526	3.73832E-47	42(3, 39) → 42(3, 39)	268.4731
23	18.3	117.62	8.72	0.2192	938.1758	1.29104E-45	51(2, 49) → 49(3, 47)	382.9722
24	5.6	97.19	4.87	0.4183	319.0226	3.53076E-43	56(4, 53) → 58(3, 55)	470.4185

to the gas pressure. For the CO₂ detection parameters assumed above, the on-axis two-photon excitation rate will match the collisional dephasing rate for a gas pressure of 4.4 torr, where the pressure broadening of the transition will have a HWHM of 13 MHz.

In order to efficiently build up the intracavity power, we need to lock the excitation laser to the cavity (or visa versa) with a relative frequency jitter of much less than the width of the cavity mode, which has a FWHM of $\gamma_1/2\pi$, which is 9.5 kHz for the assumed cavity length and loss. Two locking schemes are considered. Galli *et al.*⁹ used the Pound-Drever-Hall method³¹ to lock a Quantum Cascade laser to their cavity with a residual laser-cavity frequency jitter well below the cavity mode width, thus demonstrating that this is technically feasible even while observing cavity decay events which interrupt the stabilization. They reported that they used an acquisition rate 2500 decays per second, very close to the 3 KHz assumed in the above calculation. In the SCAR technique, the cavity loss has to be numerically integrated to produce the predicted intensity decay curve, while TPA, without saturation, produces an analytical intensity decay curve. Thus

the computational resources required to process a TPA decay is well below that for an equivalent SCARs decay transient. An alternative approach to efficient coupling is to use optical feedback from the cavity to spontaneously lock QCL laser to the cavity.^{32,33} In this case, we would want to use 3-mirror V-shaped cavity to eliminate the reflection from the input mirror, which for identical mirror properties, will reduce the intracavity power build up by a factor of 2 due to the loss of impedance matching. However, such optical locking will likely be more tolerant of vibrations and electronic noise and thus more promising for applications outside of a laboratory setting.

V. DISCUSSION

The analysis presented in this paper has demonstrated that near-resonance, two-photon absorption of vibrational transitions, detected using a version of cavity ring-down spectroscopy, should be both highly selective and sensitive. The selectivity comes about from its Doppler-Free resonances, sparse spectrum of transitions highly enhanced by near resonances, and its unique temporal cavity decay transients which allows separation of the two-photon absorption loss from all linear or saturated loss contributions from the cavity itself or other components of the gas mixture. Quite surprisingly, at least to the author, the calculated strength of the two-photon transitions are sufficient, with near resonant enhancement, such that the sensitivity (in terms of calculated lowest detection level) is not compromised given the high power, broadly tunable, narrow linewidth, c.w. IR lasers now available, such as Quantum Cascade Lasers, and the decreasing loss of commercially available mid-IR mirrors. Crystalline Mirror Solutions has recently introduced mirrors with crystalline layers which have a measured loss $(1 - R_M) = 190$ ppm and $T_M = 144$ ppm near $4.5 \mu\text{m}$, which predicts a one-way power gain of 4000, compared to 2400 used in the above calculations.³⁴ For molecules with more complex and dense level structure than CO_2 , especially heavy asymmetric tops, a few two-photon transitions with detuning within the Doppler Width can be expected, leading to further increase in the two-photon cross section relative to state resolved one-photon absorption.

A natural question to ask is why has this not been already done? The overwhelming number of previous studies of two-photon spectroscopy have examined electronic transitions of atoms and molecules. This is perhaps not surprising in that fully allowed electronic transitions have transition dipole moments $\sim 10^2$ times larger than the corresponding vibrational transitions. In addition, high power pulsed lasers have been more readily available in the visible spectral region. There was one

attempt to observe two-photon excitation of NO₂ using CRDS, but this was unsuccessful.³⁵ The excitation region scanned in this study has extremely weak NO₂ one-photon transitions, the one photon CRDS absorption sensitivity was well below current level, and the fitting did not address the expected changes in cavity decay temporal shape, so it is difficult to judge the significance of this failure.

In the early days of mid-IR laser spectroscopy, the only readily available laser sources were fixed frequency atomic lasers (such as the IR He-Ne laser) and line tunable molecular lasers such as the CO₂, NNO, and CO lasers. These had limited tuning (limited by Doppler widths of the laser gain transitions) but had relatively high power. Relevant to the present paper, a number of IR double resonance transitions were observed, even without cavity enhancement, in molecules such as CH₃F^{36–39} and NH₃^{36,40–43} by Stark Shifting the two-photon transitions into resonance with the fixed frequency lines of a CO₂ laser.

VI. SUPPLEMENTARY MATERIAL

Tables are given as supplementary material that have listed the strongest ro-vibrational two-photon transitions of molecules, calculated using data from the HITRANonline spectral database. Two photon cross sections are calculated for a pressure of 1 torr, using the air-broadening pressure broadening coefficients from the database. The cross sections are listed for molecules in the specific initial state, for the specific isotopologue by scaling by the thermal fractional population of that state at the HITRAN reference temperature, 293 K, and per molecule of the specific chemical species by scaling by the fractional population of the isotopologue as given by database. Files in common separated value format. Separate files are given for diatomics, linear molecules, and symmetric tops.

VII. ACKNOWLEDGEMENTS

The author wishes to take Dr. Manik Pradhan of the S.N. Bose National Center for Basic Sciences for providing him with the results of his recent electronic structure calculations on trans-Butadiene, which allowed a realistic calculation of the two-photon vibrational spectrum for this molecule. He also wishes to acknowledge helpful discussions and comments by Dr. Joseph T. Hodges, of N.I.S.T. The University of Virginia is supported this work.

REFERENCES

- ¹A. O'keefe and D. A. G. Deacon, "Cavity ring-down optical spectrometer for absorption-measurements using pulsed laser sources," *Review of Scientific Instruments* **59**, 2544–2551 (1988).
- ²G. Berden and R. Engeln, eds., *Cavity Ring-down Spectroscopy: Techniques and Applications* (Blackwell Publishing, Oxford, 2008).
- ³G. Gagliardi and H.-P. Loock, eds., *Cavity-Enhanced Spectroscopy and Sensing*, Springer Series in Optical Sciences, Vol. 179 (Springer, 2014).
- ⁴S. C. Xu, G. H. Sha, and J. C. Xie, "Cavity ring-down spectroscopy in the liquid phase," *Review Of Scientific Instruments* **73**, 255–258 (2002).
- ⁵Z. Qu, J. Engstrom, D. Wong, M. Islam, and C. F. Kaminski, "High sensitivity liquid phase measurements using broadband cavity enhanced absorption spectroscopy (bbceas) featuring a low cost webcam based prism spectrometer," *Analyst* **138**, 6372–6379 (2013).
- ⁶A. C. R. Pipino, J. W. Hudgens, and R. E. Huie, "Evanescent wave cavity ring-down spectroscopy for probing surface processes," *Chemical Physics Letters* **280**, 104–112 (1997).
- ⁷H. V. Powell, M. Schnippering, M. Mazurenka, J. V. Macpherson, S. R. Mackenzie, and P. R. Unwin, "Evanescent wave cavity ring-down spectroscopy as a probe of interfacial adsorption: Interaction of tris(2,2'-bipyridine)ruthenium(ii) with silica surfaces and polyelectrolyte films," *Langmuir* **25**, 248–255 (2009).
- ⁸M. Sangwan, W. R. Stockwell, D. Stewart, and L. Zhu, "Absorption of near uv light by hno₃/no₃- on sapphire surfaces," *Journal of Physical Chemistry A* **120**, 2877–2884 (2016).
- ⁹I. Galli, S. Bartalini, R. Ballerini, M. Barucci, P. Cancio, M. De Pas, G. Giusfredi, D. Mazzotti, N. Akikusa, and P. De Natale, "Spectroscopic detection of radiocarbon dioxide at parts-per-quadrillion sensitivity," *Optica* **3**, 385–388 (2016).
- ¹⁰C. R. Bucher, K. K. Lehmann, D. F. Plusquellic, and G. T. Fraser, "Doppler-free nonlinear absorption in ethylene by use of continuous-wave cavity ringdown spectroscopy," *Applied Optics* **39**, 3154–3164 (2000).
- ¹¹G. Giusfredi, S. Bartalini, S. Borri, P. Cancio, I. Galli, D. Mazzotti, and P. De Natale, "Saturated-absorption cavity ring-down spectroscopy," *Physical Review Letters* **104**, 110801 (2010).
- ¹²K. K. Lehmann, "Theoretical detection limit of saturated absorption cavity ring-down spectroscopy (scar) and two-photon absorption cavity ring-down spectroscopy," *Applied Physics B-*

- Lasers and Optics **116**, 147–155 (2014).
- ¹³L. S. Vasilenko, V. P. Chebotaev, and A. V. Shishaev, “Line shape of 2-photon absorption in a standing-wave field in a gas,” *Jetp Letters-Ussr* **12**, 113–116 (1970).
- ¹⁴B. Cagnac, G. Grynberg, and F. Biraben, “Multiphotonic absorption spectroscopy without doppler broadening,” *Journal De Physique* **34**, 845–858 (1973).
- ¹⁵F. Biraben, B. Cagnac, and G. Grynberg, “Experimental evidence of 2-photon transition without doppler broadening,” *Physical Review Letters* **32**, 643–645 (1974).
- ¹⁶F. Biraben, “The first decades of doppler-free two-photon spectroscopy,” *Comptes Rendus Physique* (2019).
- ¹⁷M. Göppert-Mayer, “ÜIJber elementarakte mit zwei quantensprüngen,” *Annalen der Physik* **401**, 273–294 (1931).
- ¹⁸H. Mahr, “Two-photon absorption spectroscopy,” in *Quantum Electronics: A Treatise*, Vol. 1, edited by H. Rabin and C. Tang (Academic Press, 1975) pp. 285–361.
- ¹⁹W. M. McClain and R. Harris, “Two-photon molecular spectroscopy in liquids and gases,” in *Excited States*, Vol. 3, edited by E. Lim (Academic, New York, 1977) pp. 1–56.
- ²⁰J. Oreg, F. T. Hioe, and J. H. Eberly, “Adiabatic following in multilevel systems,” *Physical Review A* **29**, 690–697 (1984).
- ²¹H. C. Van de Hulst and J. J. M. Reesinck, “Line breadths and voigt profiles,” *Astrophysical Journal* **106**, 121–127 (1947).
- ²²K. D. Bonin and T. J. McIlrath, “2-photon electric-dipole selection-rules,” *Journal of the Optical Society of America B-Optical Physics* **1**, 52–55 (1984).
- ²³W. M. McClain, “Excited state symmetry assignment through polarized 2-photon absorption studies of fluids,” *Journal of Chemical Physics* **55**, 2789–2796 (1971).
- ²⁴C. Townes and A. Schawlog, *Microwave Spectroscopy* (Dover, 1955) table 4.4.
- ²⁵A. Yariv, *Quantum Electronics*, 2nd ed. (John Wiles & Sons, New York, 1975).
- ²⁶I. E. Gordon, L. S. Rothman, C. Hill, R. V. Kochanov, Y. Tan, P. F. Bernath, M. Birk, V. Boudon, A. Campargue, K. V. Chance, B. J. Drouin, J. M. Flaud, R. R. Gamache, J. T. Hodges, D. Jacquemart, V. I. Perevalov, A. Perrin, K. P. Shine, M. A. H. Smith, J. Tennyson, G. C. Toon, H. Tran, V. G. Tyuterev, A. Barbe, A. G. Császár, V. M. Devi, T. Furtenbacher, J. J. Harrison, J. M. Hartmann, A. Jolly, T. J. Johnson, T. Karman, I. Kleiner, A. A. Kyuberis, J. Loos, O. M. Lyulin, S. T. Massie, S. N. Mikhailenko, N. Moazzen-Ahmadi, H. S. P. Müller, O. V. Naumenko, A. V. Nikitin, O. L. Polyansky, M. Rey, M. Rotger, S. W. Sharpe, K. Sung, E. Starikova, S. A. Tashkun,

- J. V. Auwera, G. Wagner, J. Wilzewski, P. Wcisłó, S. Yu, and E. J. Zak, “The HITRAN2016 molecular spectroscopic database,” *Journal of Quantitative Spectroscopy and Radiative Transfer* **203**, 3–69 (2017).
- ²⁷K. Podgorski, E. Terpetschnig, O. P. Klochko, O. M. Obukhova, and K. Haas, “Ultra-bright and -stable red and near-infrared squaraine fluorophores for in vivo two-photon imaging,” *Plos One* **7**, e51980 (2012).
- ²⁸(2019), <https://hitran.org/>.
- ²⁹S. Maithani, A. Maity, and M. Pradhan, “High-resolution spectral analysis of hybrid A/B-type band of 1,3-butadiene at 6.2 μm using an EC-QCL coupled with cavity ring-down spectroscopy,” *Chemical Physics* **522**, 123–128 (2019).
- ³⁰H. Huang and K. K. Lehmann, “Sensitivity limit of rapidly swept continuous wave cavity ring-down spectroscopy,” *Journal Of Physical Chemistry A* **115**, 9411–9421 (2011).
- ³¹R. W. P. Drever, J. L. Hall, F. V. Kowalski, J. Hough, G. M. Ford, A. J. Munley, and H. Ward, “Laser phase and frequency stabilization using an optical-resonator,” *Applied Physics B-Photophysics and Laser Chemistry* **31**, 97–105 (1983).
- ³²B. Dahmani, L. Hollberg, and R. Drullinger, “Frequency stabilization of semiconductor lasers by resonant optical feedback,” *Opt. Lett.* **12**, 876–878 (1987).
- ³³E. R. T. Kerstel, R. Q. Iannone, M. Chenevier, S. Kassi, H. J. Jost, and D. Romanini, “A water isotope (^2H , ^{17}O , and ^{18}O) spectrometer based on optical feedback cavity-enhanced absorption for in situ airborne applications,” *Applied Physics B-Lasers And Optics* **85**, 397–406 (2006).
- ³⁴Private Communication from Prof. Oliver H. Heckl, June 22, 2019.
- ³⁵D. Romanini, P. Dupre, and R. Jost, “Non-linear effects by continuous wave cavity ring-down spectroscopy in jet-cooled NO_2 ,” *Vibrational Spectroscopy* **19**, 93–106 (1999).
- ³⁶W. K. Bischel, P. J. Kelly, and C. K. Rhodes, “Collisional studies of $^{12}\text{CH}_3\text{F}$ using doppler free 2 photon absorption techniques,” *Ieee Journal of Quantum Electronics* **11**, D24–D25 (1975).
- ³⁷W. K. Bischel, P. J. Kelly, and C. K. Rhodes, “Observation of doppler-free 2-photon absorption in ν_3 bands of CH_3F ,” *Physical Review Letters* **34**, 300–303 (1975).
- ³⁸W. K. Bischel, P. J. Kelly, and C. K. Rhodes, “High-resolution doppler-free 2-photon spectroscopic studies of molecules .1. ν_3 bands of $^{12}\text{CH}_3\text{F}$,” *Physical Review A* **13**, 1817–1828 (1976).
- ³⁹D. Prosnitz, R. R. Jacobs, W. K. Bischel, and C. K. Rhodes, “Stimulated-emission at 9.75 μm following 2-photon excitation of methyl-fluoride,” *Applied Physics Letters* **32**, 221–223 (1978).

- ⁴⁰W. K. Bischel, R. R. Jacobs, and C. K. Rhodes, "Doppler-free 2-photon resonances in ν_2 bands of $^{14}\text{NH}_3$ at high stark fields," *Physical Review A* **14**, 1294–1295 (1976).
- ⁴¹W. K. Bischel, P. J. Kelly, and C. K. Rhodes, "High-resolution doppler-free 2-photon spectroscopic studies of molecules .2. ν_2 bands of $^{14}\text{NH}_3$," *Physical Review A* **13**, 1829–1841 (1976).
- ⁴²J. Bokor, W. K. Bischel, and C. K. Rhodes, "Doppler-free spectroscopy of the ν_2 band in $^{14}\text{NH}_3$ - application to $16\mu\text{m}$ generation," *Journal of Applied Physics* **50**, 4541–4544 (1979).
- ⁴³R. R. Jacobs, D. Prosnitz, W. K. Bischel, and C. K. Rhodes, "Laser generation from 6 to $35\mu\text{m}$ following 2-photon excitation of ammonia," *Applied Physics Letters* **29**, 710–712 (1976).